

**ZNO NPS LOADED / KAPPA-CARRAGEENAN FILM FOR PROTECTION AGAINST UV-RADIATIONS****Aniteshma Chanpuria<sup>1</sup>, M. Bajpai<sup>2</sup>, S. K. Bajpai<sup>3</sup> and Seema Tiwari<sup>4,\*</sup>**<sup>1,2,3</sup> Polymer Research Laboratory, Department of Chemistry, Government Science College, Jabalpur, Madhya Pradesh, India<sup>4</sup> Army Institute of Technology, Dighi, Pune, Maharashtra, India<sup>4</sup>stiwari@aitpune.edu.in**ABSTRACT**

Zinc oxide nanoparticles (ZnO NPs) /Kappa Carrageen (KC) composite films have been fabricated via ionic gelation method to protect wounds from UV radiation exposure. The films were characterized by FTIR, SEM and XRD analysis. The TEM analysis revealed that ZnO nanoparticles were a mixture of rod and hexagonal shaped geometries. The characteristic peaks of ZnO NPs were obtained in XRD analysis. The films, containing 0.2 and 0.4% (w/v) of ZnO NPs, exhibited Percent Transmittance of less than 5 when exposed to UV radiations. Moreover, values of Ultraviolet Protection Factor (UPF) for these films were found to be 57.13 and 234.15 respectively. The Methylene Blue (MB) degradation study also confirmed UV protection action of these films.

*Index Terms - Carrageenan, ZnO nanoparticles, Ultraviolet Protection.*

**INTRODUCTION**

Kappa Carrageenan (KC), is an anionic linear sulphated polysaccharide, consists of alternating  $\alpha$ -1,3 galactose and  $\beta$ -1,4,3,6 anhydro galactose with one sulphate ester groups [1]. Its viscoelastic and thermo-gelling property, and presence of many functional groups (sulphate and hydroxyl) makes it a suitable candidate for biomedical applications [2-4]. The special property of KC to undergo thermal gelation makes it a better candidate for preparing hydrogel patch as compared to other biopolymers/synthetic polymers which require some chemical reactions to yield a stable hydrogel. In fact, KC has so many advantageous features: (i) it has wound healing property, (ii) it undergoes thermal gelation (iii) no toxic chemicals are required to prepare polymeric film, (iv) any bioactive ingredient can conveniently be incorporated into KC film just by mixing the ingredient into pre-gel forming solution under normal stirring, and finally, the stability of KC film can be enhanced by carrying out its ionic crosslinking using KCl. Recent past has witnessed tremendous research work on polysaccharides-based hydrogel patches that have been fabricated to manage wound healing process [5,6]. Indeed, these dressings are quite successful in wound healing. However, the people, residing in high altitude areas, have high UV exposure and their skin suffers from some additional complications such as sunburn inflammation (erythema), tanning, and local or systemic immune suppression. At the molecular level, UV irradiation causes DNA damage such as cyclobutane pyrimidine dimers and photo products [7] which are usually repaired by nucleotide excision repair (NER). Therefore, apart from bacterial infection and other related disorders, adverse effects of UV radiation penetration on the infected skin also needs to be considered while developing hydrogel patches. Hence, it is desirable to prepare a hydrogel with protective ability against UV exposure. As the third-generation semiconductor material, ZnO nanoparticles have a forbidden band width of 3.37eV, a high transmittance for the visible light band and a strong absorption for the ultraviolet band due to its wide energy band gap (3.37eV that corresponds to 376 nm).

Thus, looking to the above highlighted properties of polymer Carrageenan and ZnO nanoparticles, we hereby propose a hydrogel patch, composed of natural polysaccharide Kappa Carrageenan, well-dispersed ZnO nanoparticles. The novelty of the work lies in the facts that: (i) A detailed investigation, perhaps for the first time, has been carried out to test the UV protection efficiency of the patch by using a dye-degradation method, (ii) various mixtures of UV and visible radiations in different proportions (as may be found in high altitude areas of a country) have also been employed while conducting UV protection experiments.

**EXPERIMENTAL****2.1 Materials****• Kappa-Carrageenan (KC)**

Kappa-Carrageenan (Irish moss) with high molecular mass was purchased from Hi Media Chemicals, Mumbai, India and used as received.

**• Zinc Chloride (ZnCl<sub>2</sub>)**

Zinc Chloride (Hi Media Chemicals, Mumbai, India) with molecular mass 136.286 g/mol was G.R. grade and used as received.

**• Sodium Hydroxide (NaOH)**

Sodium hydroxide (Hi Media Chemicals, Mumbai, India) with molecular mass 39.997 g/mol was G.R. grade and used as received.

**• Potassium Chloride (KCl)**

Potassium Chloride, readily dissolves in water and having molecular mass 74.551 g/mol was purchased from Hi Media Chemicals, Mumbai, India and used as received.

**• Water**

The double distilled water was used in all the experiments.

**2.2 Preparation of K<sup>+</sup> Ions Crosslinked plain KC Film**

50 ml of 1.6 % (w/v) solution of KC was taken in a beaker and to this 1 ml of glycerol was added under mild stirring at 70°C till a uniform transparent solution was obtained. Now, the above solution was poured into a Petri plate and allowed to cool. The resulting film, obtained due to the thermal gelation, was carefully removed and poured into 250 ml of a 3% (w/v) KCl solution for 60 minutes to allow the ionic crosslinking. The cross-linked film was dried in a dust-free chamber at room temperature.

**2.3 Preparation of ZnO Nanoparticles**

ZnO nanoparticles were prepared by co-precipitation method as reported elsewhere [8]. For this, 100 ml of 1.0 M ZnCl<sub>2</sub> solution was prepared in distilled water and 2% (w/v) NaOH solution was added drop-wise under constant stirring. The white precipitate of Zn (OH)<sub>2</sub>, thus obtained, was filtered and transferred into Watch glass and kept in an electric oven (Tempstar, India) at 110°C for a period of 6 h. The ZnO nanoparticles, so produced, were kept in a dust-free chamber for further use. The overall formation of Zinc Oxide (ZnO) nanoparticles can be illustrated by a scheme shown in Fig.1.

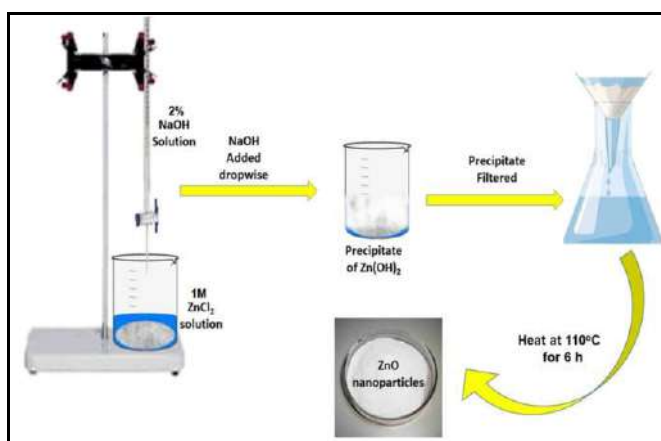


**Figure 1.** The Scheme Showing Formation of ZnO Nanoparticles.

## 2.4 Sonication of ZnO Nanoparticles

To make ZnO nanoparticles loaded polymeric film, it is necessary that the ZnO nanoparticles are uniformly dispersed in the polymeric film and to form well dispersed ZnO nanoparticles loaded polymeric film, by sonication process, prepared a suspension solution of ZnO nanoparticles. For this, adding 200mg of ZnO nanoparticles in 50 ml of distilled water and sonicated it for 30 minutes

## 2.5 Preparation of ZnO NPs-loaded KC film

In a typical protocol, 50 ml of ZnO nanoparticles suspension solution was taken in a beaker and to this 0.8g of KC and 1 ml of glycerol was added under mild stirring at 70°C till a uniform dispersion was obtained. Now, the above solution was poured into a Petri plate and allowed to cool. The resulting film, obtained due to the thermal gelation, was taken out carefully and poured into 250 ml of a 3% KCl (w/v) solution for 60 min to allow the ionic crosslinking. The cross-linked film was dried in a dust-free chamber at room. Fig.6. Overall scheme for the preparation of composite film (ZnO NPs loaded/KC) is shown.

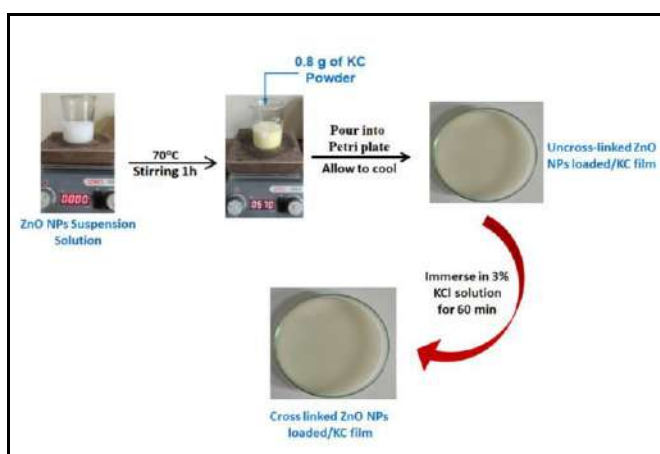


**Figure 2.** Overall Scheme for the Preparation of Composite Film Cross-Linked (ZnO NPs-Loaded/KC) is Shown.

**Table.1.** Composition of Various Films Prepared. The representative sample is designated as: FZn<sub>x</sub> F = 1.6% Kappa carrageenan cross-linked with 3% (w/v) KCl solution

Sample Code	Amounts of various Constituents		
	Carrageenan % (w/v)	ZnO nanoparticles % (w/v)	KCl % (w/v)
FZn <sub>0,0</sub>	1.6	0.0	3.0
FZn <sub>0,1</sub>	1.6	0.1	3.0
FZn <sub>0,2</sub>	1.6	0.2	3.0
FZn <sub>0,4</sub>	1.6	0.4	3.0
FZn <sub>0,6</sub>	1.6	0.6	3.0
FZn <sub>0,8</sub>	1.6	0.8	3.0

Where, the number  $x$  in subscript, denote the wt. % of ZnO NPs and symbol F represents a Carrageenan film composed of 1.6 % (w/v) Carrageenan and 4 percent (v/v) glycerol and crosslinked with 3 %(w/v) of KCl solution.

## 2.6 CHARACTERIZATION

### 2.6.1 FT-IR Analysis

The infrared spectrum of absorption of a solid is obtained by Fourier Transform Infrared Spectrophotometer (Shimadzu, 8400, Japan). The powdered form of plain  $K^+$  ions crosslinked Carrageenan, ZnO NPs and ZnO NPs loaded/KC samples were analysed. And powdered sample was mixed with KBr, the scan was recorded, and the selected spectral range was in between 400 to 4000  $cm^{-1}$ .

### 2.6.2 XRD Analysis

The Crystallinity Index of the ZnO nanoparticles was measured by X-Ray diffraction method, the XRD analysis was carried out a Rikagu diffractometer (Cu radiation = 0.1546 nm), running at 40 KV and 40 mA. ZnO nanoparticles were imaged at 200 X using on Olympus 1X 71 microscopes equipped with a DP 71 camera (Olympus Corporation, Tokyo, Japan).

### 2.6.3 TEM Analysis

The structure of ZnO nanoparticles was determined by using Transmission Electron Microscopy (TEM JEOL 1010). For observation the ZnO nanoparticles suspensions placed to the Copper grids coated with a carbon supported film. The TEM images of ZnO nanoparticles were obtained without any sample staining.

### 2.6.4 SEM Analysis

The surface morphology of the plain  $K^+$  ions crosslinked Carrageenan film and ZnO NPs loaded/KC composite film was determined by Scanning Electron Microscope analysis by using JEOL 6400 F microscope, The accelerating voltage of 2 KV and a working distance of 4.4 mm with a 50  $\mu$ L sediment suspension were sprayed silicon wafers to clean them followed by air drying for 24 hours, and then being coated with an approximately 6 nm layer of gold and palladium.

## 2.7 UV-Blocking Property of Films

### 2.7.1 UV Protection Efficiency of ZnO Nanoparticles-loaded Film

For this experiment different concentrations of ZnO nanoparticles loaded Kappa- Carrageenan composite film samples cut into size of wall of cuvette and placed in the path of the UV lamp for various wavelengths radiation. The % transmittance of the film recorded and graph plotted between incident wavelength and corresponding % transmittance.

### 2.7.2 UV-Blocking Capacity of Films and UPF Measurement

The Ultraviolet Protection Factor (UPF) was determined following the procedure described elsewhere [9]. In brief, films were cut into rectangular pieces, matching the wall of the quartz cuvette, placed across the wall and transmittance was recorded in the wavelength range of 280 to 400 nm.

The UPF was calculated using the following expression:

$$UPF = \frac{\sum_{280}^{400} E_{\lambda} S_{\lambda} \Delta\lambda}{\sum_{280}^{400} E_{\lambda} S_{\lambda} T_{\lambda} \Delta\lambda} \dots \quad (1)$$

Where,

$E_{\lambda}$  = Relative erythemal spectral effectiveness

$S_{\lambda}$  = Solar spectral irradiance in  $W. m^{-2} .nm^{-1}$

$T_{\lambda}$  = Spectral transmittance  $\Delta\lambda$  = wavelength

step in nm  $\lambda$  = wavelength in nm

The percent blocking (PB) for UV-A and UV-B radiations, in the range of 320-400 nm and 280-320 nm respectively, was determined from following equations:

$$(PB)_{UV-A} = 100 - \frac{\sum_{320}^{400} T_{\lambda} d\lambda}{\sum_{320}^{400} d\lambda} \dots \quad (2)$$

$$(PB)_{UV-B} = 100 - \frac{\sum_{280}^{320} T_{\lambda} d\lambda}{\sum_{280}^{320} d\lambda} \dots \quad (3)$$

### 2.8 Methylene Blue Photodegradation Method

UV radiations blocking action of films was also confirmed by carrying out photo degradation of Methylene Blue solution by UV/H<sub>2</sub>O<sub>2</sub> [10]. In brief, 25 ml of MB solution of known concentration, containing 1 ml of H<sub>2</sub>O<sub>2</sub>, was taken in a beaker and placed in a thermostatic shaker. The mouth of beaker was covered with film samples FZn<sub>0.0</sub>, FZn<sub>0.1</sub>, FZn<sub>0.2</sub>, and FZn<sub>0.4</sub>, and UV light was allowed to pass through the top as shown in Fig.3. The absorbance was recorded periodically to measure the extent of degradation.

$$\% \text{ Degradation} = \frac{\text{Initial absorbance} - \text{Time 't' absorbance}}{\text{Initial absorbance}} \times 100 \quad (4)$$

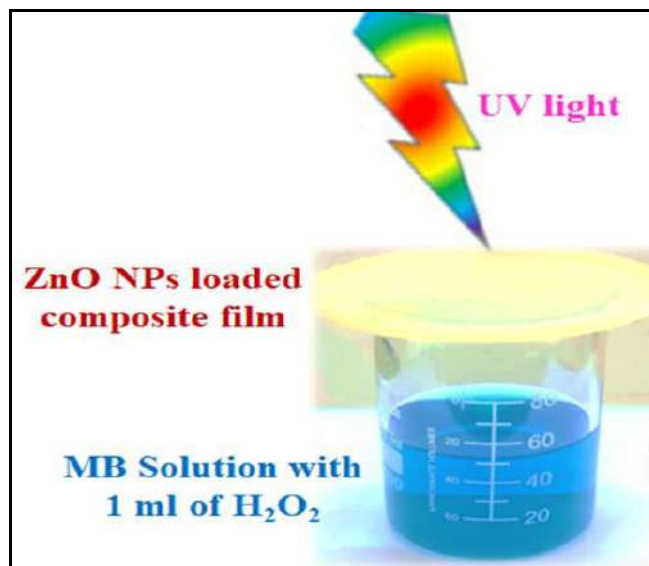


**Figure 3.** Schematic Diagram for Photodegradation of Methylene Blue Solution by ZnO Nps Loaded/Kc Film Sample.

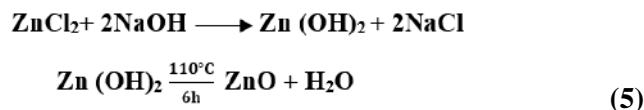
## RESULT AND DISCUSSION

### 3.1. Preparation of K<sup>+</sup> Ions Cross-linked Plain KC Film

When thermally gelled KC film is immersed in the KCl aqueous solution, K<sup>+</sup> ions enter into the film matrix and occupy place within the double helical structures to counter the negatively charged sulphate groups [11]. As the distance between the two-hydrogen bonded in double helices is almost 0.3 nm and the size of potassium ions is 0.26 nm, the approach of K<sup>+</sup> ions is highly probable to occupy the junction points to produce cross linked matrix.

### 3.2 Synthesis of ZnO Nanoparticles

ZnO nanoparticles were prepared by Co-precipitation method [12-14]. When 2% (w/v) solution of NaOH is added drop-wise to aqueous solution of ZnCl<sub>2</sub>, white precipitate of Zn (OH)<sub>2</sub> is obtained. When this precipitate is heated at 110°C, ZnO nanoparticles are obtained. By following well known reaction:



### 3.3 Preparation of ZnO NPs-loaded KC film

When a hot aqueous solution of KC, containing definite amount of well dispersed ZnO NPs, is poured into Petri plate and allowed to cool, there occurs a conformational change from random coil to single helices, followed by formation of double helices. These double helices aggregate to produce a three-dimensional structure [15]. During this process, the well-dispersed ZnO nanoparticles are uniformly entrapped within the Carrageenan macromolecular network, thus resulting in formation of ZnO NPs loaded /KC film matrix.

### 3.4 CHARACTERIZATION

#### 3.4.1 FT-IR Analysis

In FTIR spectrum of sample FZn<sub>0.0</sub> (KCl cross linked KC film), Fig.4. (a) a peak at 1010 cm<sup>-1</sup> confirms the glycosidic linkage and band at 1270 cm<sup>-1</sup> is ascribed to the sulphate group. The OH stretching vibration is also observed in the region of 3000cm<sup>-1</sup> to 3600cm<sup>-1</sup>. The FTIR spectrum of ZnO NPs, depicted in Fig.4. (b), shows an absorption peak at 460 cm<sup>-1</sup> which confirms the metal-oxygen bonding (ZnO stretching vibrations) [16]. Finally, in the spectrum of ZnONPs loaded/KC composite film (FZn<sub>0.4</sub>), shown in Fig.4. (c), A band appearing at 450-520 cm<sup>-1</sup> and 1010cm<sup>-1</sup> indicates the presence of Zn-O bond and glycosidic bond which are also present in spectra of pure ZnO nanoparticles and KC respectively.

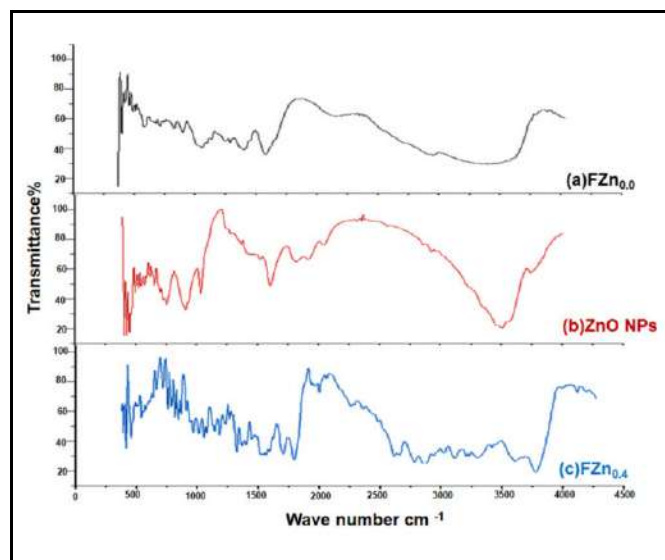


**Figure 4.** Ftir Spectrum of (A) Plain Kcl Crosslinked Kc Film Fzn0.0 (B)Native Zno Nps and (C) Zno Nps Loaded/Kc Film Fzn0.4 (Defence Institute of Advance Technology, Pune).

#### 3.4.2 The Surface Plasmon Resonance (SPR)

The SPR of ZnO nanoparticles were also recorded as shown in Fig.5. A broad absorption peak is observed at 356 nm which indicates that ZnO nanoparticles has relatively bigger size and no spherical geometry.

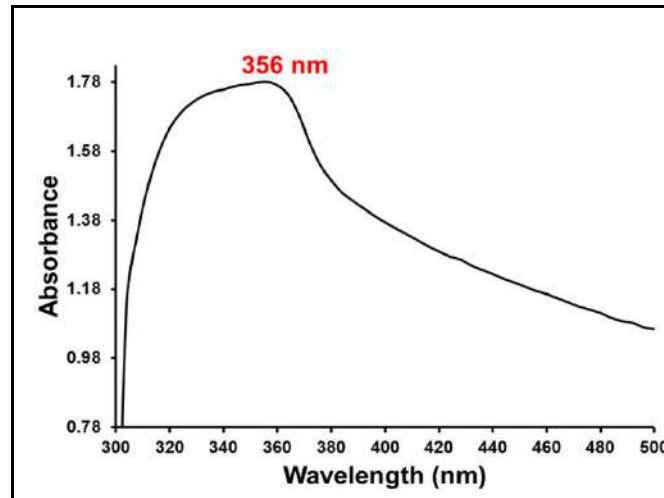


Figure 5. The Spr Spectrum of ZnO Nanoparticles at Room Temperature.

### 3.4.3 XRD Analysis of ZnO Nanoparticles

The XRD pattern of ZnO nanoparticles, Fig.6. exhibits diffraction peaks at  $31.81^\circ$ ,  $34.59^\circ$ ,  $36.38^\circ$ ,  $47.67^\circ$ ,  $56.67^\circ$ ,  $62.98^\circ$ ,  $68.19^\circ$  and  $69.11^\circ$ , which correspond to reflection at (100), (002), (101), (102), (110), (103), (200) and (112) respectively, thus suggesting hexagonal Wurtzite phase.

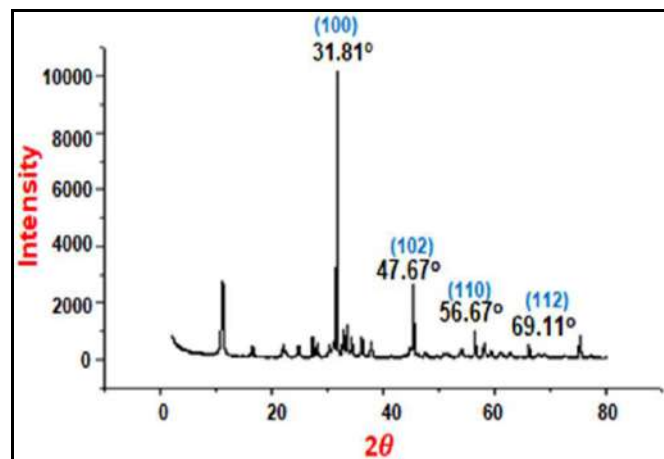
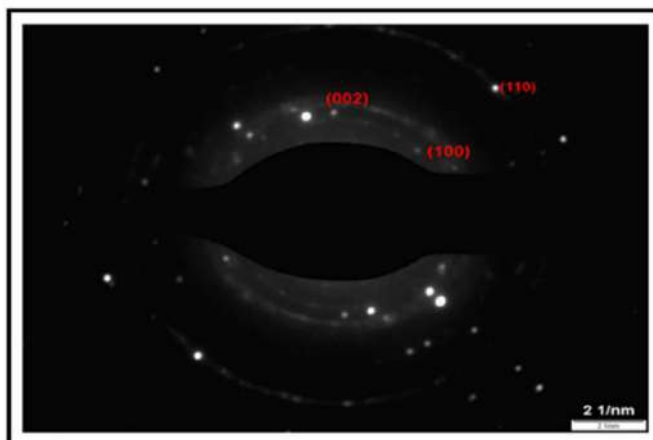


Figure 6. X-Ray Diffractogram of ZnO Nanoparticles (Defence Institute of Advance Technology, Pune).

### 3.4.4 SAED Pattern of ZnO Nanoparticles

The SAED pattern, shown in Fig.7., shows bright spots, forming rings of different radii, over a bar length of 5  $1/\text{nm}$ . These spots, arranged in rings, also indicate the presence of plentiful well defined nano crystallites. The radii of various rings were measured and transformed into inter-planar distance 'd' ( $=1/R$ ). These spacing, when compared with the standard data available, enabled us to identify the respective planes, namely (100), (002) and (110).



**Figure 7.** Saed Pattern of ZnO Nanoparticles (Defence Institute of Advance Technology, Pune).

### 3.4.5 TEM Analysis of ZnO Nanoparticles

The TEM image, shown in Fig.8 (a), indicates that most of the nanoparticles have rod shaped geometry while some irregular shaped, rather hexagonal, are also visible, thus indicating that a mixture of different geometries has been obtained. This is further supported by Fig.8 (b) in which a cluster of rod-shaped nanoparticles is seen along with some big sized irregular shaped particles. The presence of hexagonal and rod-shaped particles is further confirmed in the Fig.8 (c) and (d) respectively. Indeed, geometry of ZnO nanoparticles depend upon the method of preparation also. For example [17] used sol-gel method and found that their geometries varied from spherical to rod-like, with an average particles size of around 38 nm. The particles had a tendency to agglomerate due to calcinations. However, the hydrothermal approach yielded plate-like shaped particles with a diameter of 162 nm and thickness of 10 to 18 nm. Moreover, Polyol method yielded polyhedron type shape with no agglomerations.

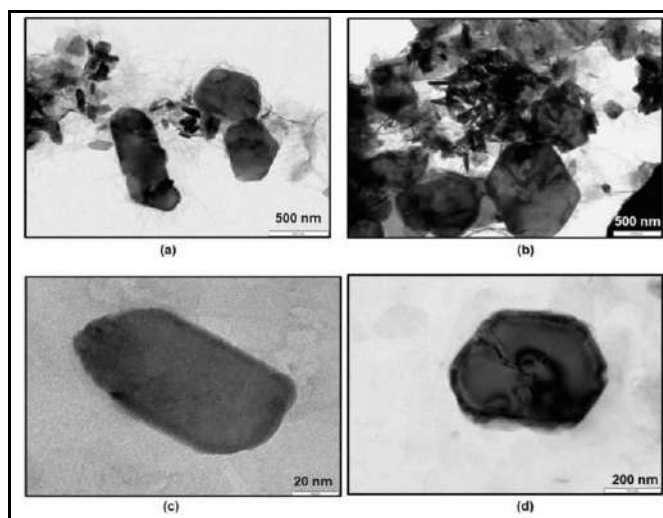


**Figure 8.** Tem Images of ZnO Nanoparticles with Different Magnifications (Saif, Iit Bombay).

### 3.4.6 SEM Analysis of Film Samples

The SEM images of samples FZn<sub>0,0</sub> and FZn<sub>0,4</sub> with 1000 X magnifications are shown in Fig.9. (a) and (b) respectively. It can clearly be seen in Fig.9. (a) that plain KC film contains aggregated Carrageenan particles distributed uniformly throughout the matrix. The observed agglomerations may be due to some partially dissolved KC particles. The surface texture of ZnO NPs loaded/KC film, as shown in Fig.9. (b), reveals presence of uniformly dispersed ZnO NPs.

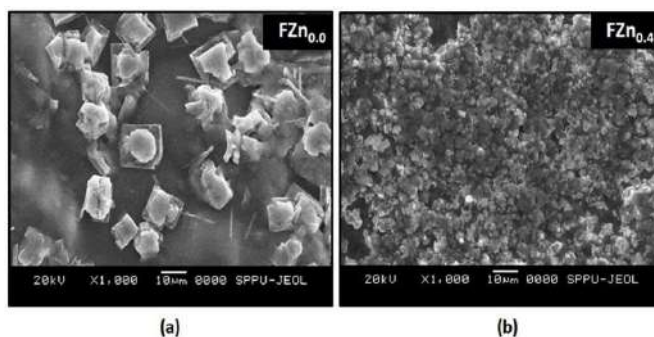


**Figure 9.** Sem Images Of (A) Plain Kcl Crosslinked Carrageenan Film Fzn0.0 (B) ZnO Nps Loaded/Kc Film Fzn0.4 (Defence Institute of Advance Technology, Pune).

### 3.5 UV BLOCKING PROPERTY OF FILMS

#### 3.5.1 UV Protection Efficiency of Films

In order to investigate the protection efficiency of ZnO nanoparticles in composite hydrogel films, we prepared a number of hydrogel film samples containing different quantities of ZnO nanoparticles in the range of 0 mg to 200 mg and determine their % transmittance, as depicted in Table 2 and Fig.10., reveal that as ZnO nanoparticles content increases from 0 mg to 200 mg the % transmittance decreases 61.7% to 1% that means 200 mg ZnO nanoparticles loaded/KC film blocks 99% of UV radiation.

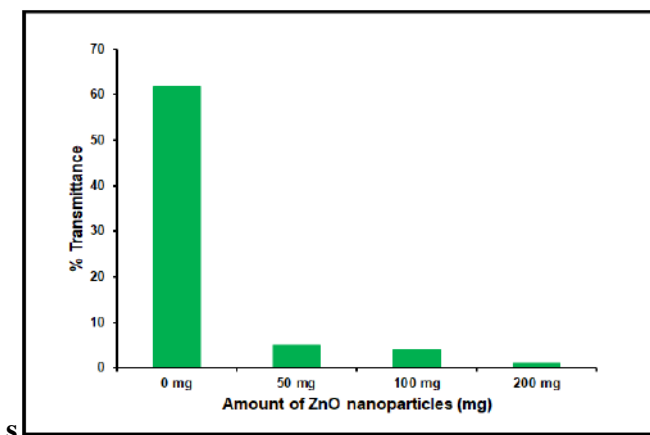


**Figure 10.** Bar Diagram Showing % Transmittance for Composite Films Containing Different Quantities of ZnO Nps At 37oc.

**Table.2.** Data Showing % Transmittance for Composite Films Containing Different Quantities of ZnO Nps.

Samples	% Transmittance
FZn <sub>0.0</sub>	61.7%
FZn <sub>0.1</sub>	4.9%
FZn <sub>0.2</sub>	4.0%
FZn <sub>0.4</sub>	1.0%

#### 3.5.2 UV Blocking Capacity of Films and UPF Measurement

Because of wide energy band gap, ZnO nanoparticles are commonly employed for blocking UV radiations [18,19]. The mechanism of UV protection efficiency by ZnO nanoparticles is shown in Fig.11. UV radiations have been classified as UV-C, UV-B and UV-A, with the irrespective range 200-280 nm, 280-320 nm and 320-400 nm [20]. As UV-C, the shortest wavelengths radiations (and so highly energetic and damaging) are absorbed by ozone layer in the atmosphere, they are unable to reach the earth and hence they were not considered in this

work. The results of UV exposure of samples FZn<sub>0,0</sub>, FZn<sub>0,1</sub>, FZn<sub>0,2</sub>, and FZn<sub>0,4</sub>, in the wavelength range of 280 to 400nm for a period of 5 min are shown in Fig.12. The sample FZn<sub>0,0</sub>, fails to block the radiations, while FZn<sub>0,1</sub>, blocks 40% in UV-A region while fails to further stop the radiations. However, the samples FZn<sub>0,2</sub>, and FZn<sub>0,4</sub> show more than 95 and 99% blocking of UV-A and UV-B radiations, thus proving their strong candidature as UV blockers. The percentage blocking and UPF values are given in Table 3. It is clear that samples FZn<sub>0,2</sub>, and FZn<sub>0,4</sub> have excellent protection efficiency.

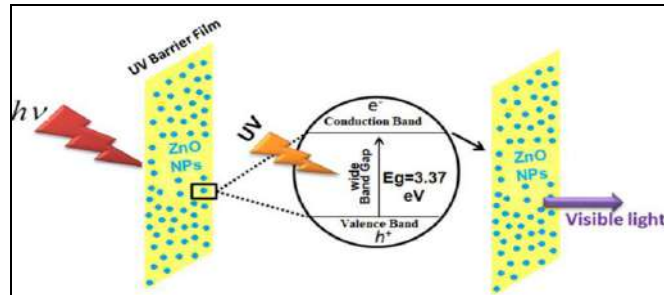


Figure 11. Scheme Showing UV Blocking Action of ZnO Nanoparticles.

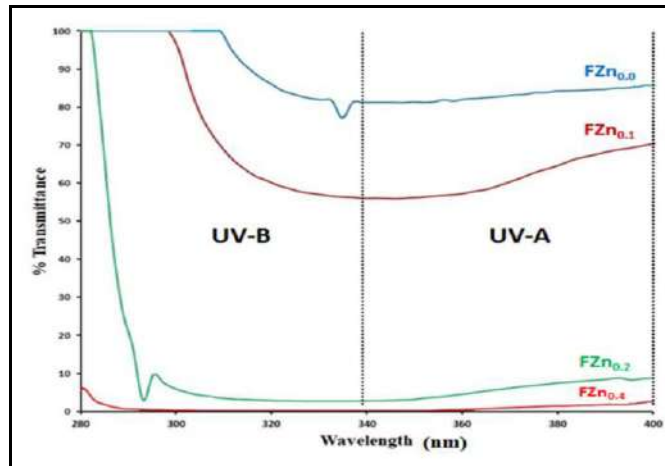


Figure 12. Transmittance Spectra for Various Film Samples in the Range of 280 To 400 Nm At 37oc.

Table.3. Data Showing Values of Upf and Percentage Blocking for the Hydrogel Films Containing Different Concentrations of ZnO Nps.

Sample code	Percentage Blocking		UPF Value
	UV-A	UV-B	
FZn <sub>0,0</sub>	26.05	6.13	1.00
FZn <sub>0,1</sub>	58.88	17.14	1.00
FZn <sub>0,2</sub>	95.41	83.71	57.09
FZn <sub>0,4</sub>	99.59	98.87	234.68

3.6. Methylene Blue Photodegradation Method

The results of photo degradation of MB in the presence of UV light are shown in Table 4 and Fig.13. It can be noticed that almost 60% degradation of MB takes place in 105 min when radiations were passed through the sample FZn<sub>0,0</sub> while in the same time period, only 26.6, 20.7, 19.5, 0.82 and 0.85% degradation of MB took place in the presence of samples FZn<sub>0,1</sub>, FZn<sub>0,2</sub>, FZn<sub>0,4</sub>, FZn<sub>0,6</sub> and FZn<sub>0,8</sub>. This may be explained on the basis of the fact that for the sample FZn<sub>0,0</sub> (which does not contain ZnO nanoparticles within the matrix), the UV radiation, passing through it, passes through the film and causes an appreciable degradation of dye MB. However, film samples

FZn<sub>0.1</sub>, FZn<sub>0.2</sub>, FZn<sub>0.4</sub>, FZn<sub>0.6</sub> and FZn<sub>0.8</sub>, which contain ZnO nanoparticles within the matrix, block most of the UV radiation passing through them and therefore less quantity of UV radiation reaches the MB solution to cause its degradation. As a result, 26.6, 20.7, 19.5, 0.82 and 0.85% degradation take place in 105 min. This further confirms UV blocking action of ZnO NPs loaded/KC films.

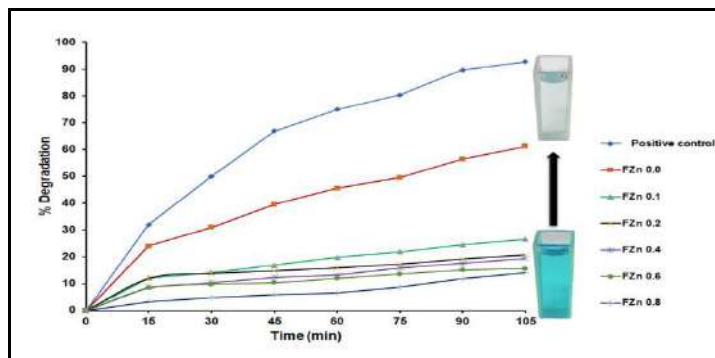


Figure 13. Degradation of MB by UV Radiations after Passing Through Various Films, At 37oc.

Table.4. Data Showing % Degradation of Methylene Blue When Exposed to Radiations Passing through Hydrogel Films With Different Zno Nps Concentrations.

Time (min)	Methylene Blue degradation by radiation passing through different films						
	Positive control	FZn <sub>0.0</sub>	FZn <sub>0.1</sub>	FZn <sub>0.2</sub>	FZn <sub>0.4</sub>	FZn <sub>0.6</sub>	FZn <sub>0.8</sub>
15	32.00	24.00	12.20	12.04	08.90	0.95	0.91
30	50.00	31.00	14.20	13.80	10.40	0.94	0.89
45	67.00	39.60	17.09	14.83	12.40	0.93	0.88
60	75.00	45.60	19.87	15.96	13.20	0.92	0.87
75	80.40	49.60	21.93	17.30	15.90	0.86	0.85
90	89.70	56.50	24.50	19.20	17.60	0.87	0.84
105	92.70	61.17	26.60	20.70	19.50	0.85	0.82

### 3.7. Real Time Monitoring of UV Exposure

In the above experiment, the radiation used to cause degradation of MB solution was of UV range only. Such a high concentration of UV light in solar radiation may probably be found in high altitude places where UV index is 10 or more. However, the places where UV index values are not so high or even moderate, solar radiation contains a limited fraction of UV light and therefore using a mixture of (UV + visible) radiations in definite proportions to cause degradation of MB solution, may reflect a more realistic picture of UV blocking action of the proposed films [21]. In the instrumentation setup, shown in Fig.14, width of slits put before the sources UV and visible light were adjusted to allow a pre-defined mixture of UV and visible radiation to pass through the film sample FZn<sub>0.6</sub> to cause degradation of MB solution. For example, to mimic UV index of 2.0, a mixture of 20% UV and 80 % visible light was employed to pass through the sample FZn<sub>0.6</sub> to induce degradation of MB solution. The results, as shown in Fig.15, indicate that as the UV index increases from 2 to 10, time required for 50% degradation decreases from 540 to 65 min respectively. In other words, when UV index is 2.0, the film sample FZn<sub>0.6</sub> is quite able to block the UV radiation and therefore a slower MB degradation is observed (time required for 50% degradation is 540 min). However, as the UV index increases, UV content in the exposed light also increases and therefore the UV blocking efficiency of sample FZn<sub>0.6</sub> begins to decrease. This experiment indicates that the concentration of ZnO nanoparticles in the film should be adjusted as per UV index value of the place where the film is intended to be used.

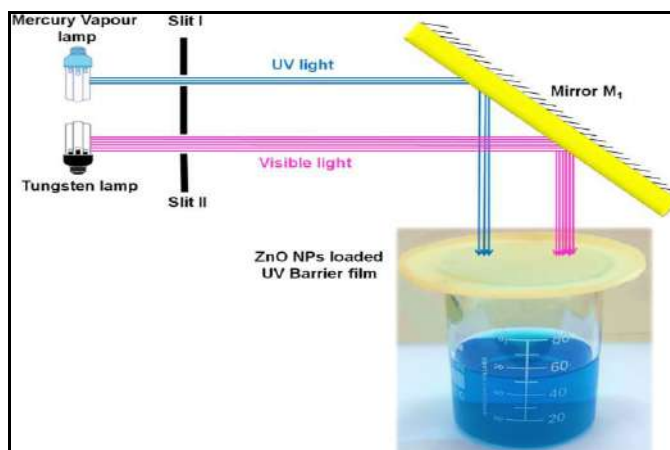


Figure 14. Schematic Diagram for UV Exposure Study.

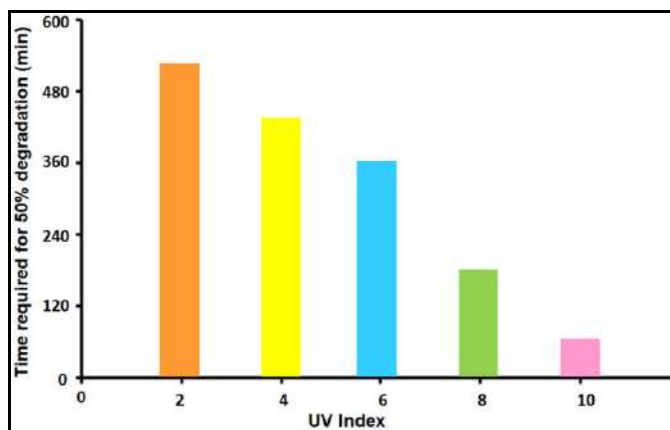


Figure 15. Bar-Diagram Showing Time Required For 50% Degradation Of Mb At Exposures of (Uv- Visible) Radiations of Varying Proportions.

## CONCLUSION

The above study concludes that ZnO nanoparticles loaded/Kappa carrageenan film shows excellent UV protection when loaded with 0.4 wt % of ZnO NPs and the patch has potential to be used for wound healing in high altitude areas where UV exposure is also a severe problem for wounded skin.

## REFERENCES

- [1] Y. Sun, B. Yang, Y. Wu, Y. Liu, X. Gu, H. Zhang, C. Wang, H. Cao, L. Huang, Z. Wang, *Food Chemistry*. **178**, 311, (2015) <https://doi.org/10.1016/j.foodchem.2015.01.105>
- [2] S. Shen, X. Chen, Z. Shen, H. Chen, *Pharmaceutics*. **13**, 1666, (2021) doi: 10.3390/pharmaceutics13101666.
- [3] Z. Noralian, M.P. Gashti, M. R. Moghaddam, H. Tayyeb, I. Erfanian, *IntJBiolMacromol*. **180**, 439, (2021) <https://doi.org/10.1016/j.ijbio.2021.02.204>.
- [4] L. Madruga, K.C. Popat, R.C. Balaban, M.J. Kipper, *Carbohydrate Polymer*. **273**, 118541, (2021). <https://doi.org/10.1016/j.carbpol.2021.118541>.

- [5] M. Arab, M. Jallab, M. Ghaffari, E. Moghbelli, & R. Saeb, *Iranian Polymer Journal*. **30**, 1019–1028, (2021). doi:10.1007/s13726-021-00952-7.
- [6] S. Feiz, A.H. Navarchian, & O.M. Jazani, *Iranian Polymer Journal*. **27**, 193, (2018). DOI:10.1007/s13726-018-0600-2.
- [7] M. Yasuhiro, N.A. Honnavara, *Toxicology and Applied Pharmacology*. **195**, 298, (2004). <https://doi.org/10.1016/j.taap.2003.08.019>.
- [8] T.R. Acharya, P. Lamichhane, R. Wahab, D.K. Chaudhary, B. Shrestha, L.P. Joshi, N.K. Kaushik, E.H. Choi, *Molecules*. **26**, 7685, (2021). <https://doi.org/10.3390/molecules26247685>.
- [9] W. Yang, S. Jing, L. Ting, M. Piming, B. Huiyu, X. Yi, C. Mingqing, *ACS Appl. Mater.* **9**, 36281, (2017). <https://doi.org/10.1021/acssuschemeng.5b01734>.
- [10] S. Liu, K. Yao, *Iranian Polymer Journal*. **26**, 681, (2017). <https://doi.org/10.1007/s13726-017-0553-x>.
- [11] J. Huang, C. Yang, Q. Song, D. Liu, L. Li, *Water SciTechnol*. **78**, 1802, (2018). <https://doi.org/10.2166/wst.2018.466>.
- [12] A.H. Farha, A.F. Naim, S.A. Mansour, *Polymers (Basel)*. **12**, 1935, (2020). <https://doi.org/10.3390/polym12091935>.
- [13] M. Gholami, M. Esmailzadeh, Z. Kachoei, M. Kachoei, B. Divband, *Biomed ResInt*. **2021**, 6397698, (2021). doi: 10.1155/2021/6397698.
- [14] G.R. Mahdavinia, S. Irvani, S. Zoroufi, & H. Hosseinzadeh, *Iranian Polymer Journal*. **23**, 335, (2014). DOI: 10.1007/s13726-014-0229-8.
- [15] Y. Deng, M. Huang, D. Sun, Y. Hou, Y. Li, T. Dong, X. Wang, L. Zhang, W. Yang *ACS Appl Mater*. **10**, 37544, (2018). <https://doi.org/10.1021/acsami.8b15385>.
- [16] M. Kaushik, R. Niranjana, V. Pandiyarasan, C. Ramachandran, G. Venkatasubbu, *Applied surface science*. **479**, 1169, (2019). <https://doi.org/10.1016/j.apsusc.2019.02.189>.
- [17] O.R. Vasile, L. Serdaru, E. Andronescu, R. Trusca, V.A. Surdu, O. Oprea, A. Ilie, B.S.Vasile, *ComptesRenduschimic*. **18**, 1335,(2015). DOI: 10.1016/j.crci.2015.01.013s
- [18] K.D. Hari, C.V. Garcia, G.H. Shin, J.T. Kim, *Polymers (Basel)*. **13**, 2403, (2021). <https://doi.org/10.3390/polym13152403>.
- [19] X. Huang, X. Zhou, Q. Dai, Z. Qin, *Nanomaterials (Basel)*. **11**, 3337, (2021). <https://doi.org/10.3390/nano11123337>.
- [20] T. Dai, M. Vrahas, C. Murray, and M. Hamblin, *Anti Infect*. **10**, 185–19, (2012). doi: 10.1586/eri.11.166 .
- [21] R. Bhattacharya, S. Pal, A. Bhoumick, P. Barman, *Int.j. of Engineering Science and Technology*. **4**, 4577, (2012). <https://doi.org/10.1155/2014/202868>.